DOI: 10.1002/chem.200701948

Theoretical Investigation of the Reaction Mechanism of the Dinuclear Zinc Enzyme Dihydroorotase

Rong-Zhen Liao,[a, b] Jian-Guo Yu,[b] Frank M. Raushel,*[c] and Fahmi Himo*[a]

Abstract: The reaction mechanism of the dinuclear zinc enzyme dihydroorotase was investigated by using hybrid density functional theory. This enzyme catalyzes the reversible interconversion of dihydroorotate and carbamoyl aspartate. Two reaction mechanisms in which the important active site residue Asp250 was either protonated or unprotonated were considered. The calculations establish that Asp250 must be unprotonated for the reaction to take place. The bridging hydroxide is shown to be capable of performing nucleophilic attack on the substrate from its bridging position and the role of Zn_β is argued to be the stabilization of the tetrahedral intermediate and the transition state leading to it, thereby lowering the barrier for the nucleophilic attack. It is furthermore concluded that the rate-limiting step is the protonation of the amide nitrogen by Asp250 coupled with C–N bond cleavage, which is consistent with previous experimental findings from isotope labeling studies.

Keywords: density functional calculations · dihydroorotase · enzyme catalysis · reaction mechanisms

Introduction

Dihydroorotase (DHO) catalyzes the reversible interconversion of dihydroorotate and carbamoyl aspartate as illustrated in Scheme 1.[1] This transformation is a key step in the de novo biosynthesis of pyrimidine nucleotides, and thus, DHO is an attractive target for inhibitor design and mechanistic interrogation.[2] Amino acid sequence comparisons have demonstrated that DHO is a member of the amidohydrolase superfamily (AHS) of enzymes.[3] The AHS is a group of enzymes that catalyze primarily hydrolytic reactions in a wide range of substrate contexts.[4] All members of the AHS possess a $(\beta/\alpha)_8$-barrel structural fold with an active site that resides at the C-terminal end of the β barrel.[4] The hydrolytic water molecule is activated for nucleophilic attack by coordination to a mononuclear or binuclear metal center. The divalent cations that have been found ligated to the active sites within these enzymes include Zn^{2+}, Ni^{2+}, and Fe^{2+}.[4] However, Mn^{2+}, Cd^{2+}, and Co^{2+} will activate some of these enzymes under certain conditions.[5]

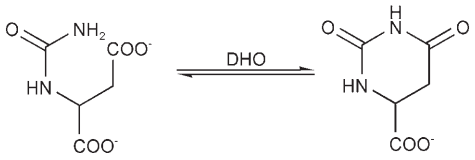

Scheme 1.

The X-ray crystal structure of DHO from *Escherichia coli* has been determined to high resolution and has a binuclear zinc cluster at the active site.[6,7] Remarkably, when the protein was crystallized in the presence of substrate at a pH at which the equilibrium constant for the enzymatic reaction was near unity, dihydroorotate was found bound to the active site of one monomeric unit of the dimeric protein, whereas carbamoyl aspartate was bound to the adjacent monomer.[6] Therefore, this crystal structure provided an almost unprecedented view of the molecular interactions between the substrate/product and the enzyme immediately

[a] R.-Z. Liao, Prof. Dr. F. Himo
Department of Theoretical Chemistry
School of Biotechnology
Royal Institute of Technology
10691 Stockholm (Sweden)
Fax: (+46) 8-5537-8590
E-mail: himo@theochem.kth.se

[b] R.-Z. Liao, Dr. J.-G. Yu
School of Chemistry
Beijing Normal University
Beijing 100875 (P.R. China)

[c] Prof. Dr. F. M. Raushel
Department of Chemistry
P.O. Box 30012
Texas A&M University
College Station, Texas 77842-3012 (USA)
Fax: (+1) 979-845-9452
E-mail: raushel@tamu.edu

before and after the chemical reaction. In DHO one of the divalent cations (M_α) is coordinated to two histidine residues from β-strand 1 and an aspartate from β-strand 8, whereas the second metal ion (M_β) is coordinated to two histidine residues from β-strands 5 and 6. In addition, the two metal ions are bridged by a carboxylated lysine from β-strand 4. In the monomer with the bound dihydroorotate, the two metal ions are further bridged by hydroxide and the carbonyl oxygen of the dihydroorotate is orientated towards M_β. Moreover, the bridging hydroxide is hydrogen bonded with the aforementioned aspartate residue from the β-strand 8. In contrast, in the monomer with a bound carbamoyl aspartate, the bridging hydroxide is missing and the two metal ions are bridged by the β-carboxylate group of the product. A representation of the active site in the presence of bound dihydroorotate is provided in Figure 1.

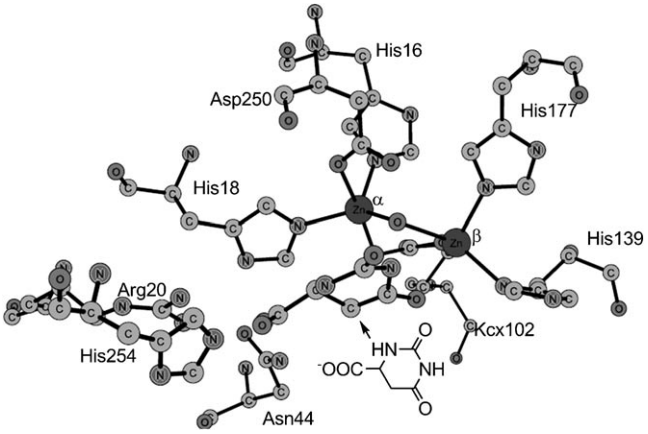

Figure 1. X-ray structure of the active site of DHO complexes with substrate dihydroorotate (coordinates taken from PDB entry 1J79).

The X-ray structure of DHO and a comprehensive assessment of the catalytic properties of this enzyme with a variety of substrates enabled Porter et al. to postulate a chemical reaction mechanism for the interconversion of dihydroorotate and carbamoyl aspartate.[8] In the hydrolysis reaction it was proposed that upon the binding of dihydroorotate the carbonyl group of the substrate was polarized by an interaction with M_β. This interaction correctly positioned the carbonyl carbon for attack by the bridging hydroxide and it weakened the interaction of the bridging hydroxide with M_β. As the hydroxide attacked the carbonyl carbon, the hydrogen-bonded proton was transferred from the hydroxide to the aspartate from β-strand 8 and a tetrahedral intermediate was formed as a bridging ligand between the two zinc ions. In the final step the tetrahedral intermediate collapsed through a concerted proton transfer from the aspartic acid residue and cleavage of the carbon–nitrogen bond. This left the newly formed carboxylate group as a bridging ligand between the two divalent cations. The key mechanistic insights from this analysis were the identification of hydrolytic nucleophile as the bridging hydroxide and the role of the aspartate residue in the shuttling of the proton from the hydroxide to the leaving-group nitrogen.[8]

In the present work, we used density functional theory (DFT) calculations to investigate the reaction mechanism of DHO. We constructed a model of the active site on the basis of the crystal structure (Protein Data Bank (PDB) entry 1J79), and employed the hybrid functional B3LYP[9] to calculate a potential-energy surface for the reaction and characterize the transition states and intermediates involved. This approach has previously been successfully applied to the study of a number of enzyme mechanisms,[10] which includes two recent studies on the reaction mechanisms of the related dizinc enzymes, phosphotriesterase (PTE)[10e] and aminopeptidase from *Aeromonas proteolytica* (AAP).[10f]

Computational Details

All calculations presented herein were carried out by means of DFT with the B3LYP functional.[9] For geometry optimization, the 6-31G(*d,p*) basis set was used for the C, N, O, and H elements and the LANL2DZ pseudopotential[11] for the zinc ions. Based on these geometries, more accurate energies were obtained by performing single-point calculations with the 6–311++G(2d,2p) basis set for all of the elements. All geometries were optimized in vacuo.

To estimate the energetic effects of the protein environment, solvation effects were calculated at the same theory level as the optimizations by performing single-point calculations on the optimized structures using the conductorlike polarizable continuum model (CPCM) method.[12] The dielectric constant (ε) was chosen to be four, which is the standard value used in modeling protein surroundings. Frequency calculations were performed at the same theory level as the optimizations to obtain zero-point energies (ZPE) and to confirm the nature of the stationary points. The latter implies no negative eigenvalues for minima and only one negative eigenvalue for transition states. As will be discussed below, some atoms were kept fixed to their X-ray crystal positions. This procedure gives rise to a few small imaginary frequencies, typically in the order of $10\,i\,cm^{-1}$. These frequencies do not significantly contribute to the ZPE and can thus be tolerated. The energies reported herein are corrected for both solvation and zero-point vibrational effects. All calculations were performed by using the Gaussian 03 program package.[13]

Active-site model: A model of the dihydroorotase active site was constructed based on the crystal structure of the enzyme complexed to dihydroorotate (PDB entry 1J79).[6] The model consists of the two zinc ions along with their ligands His16, His18, His139, His177, Asp250, and the bridging carboxylated Lys102 and hydroxide ($O_\mu H^-$). In addition, three important second-shell residues, Arg20, Asn44, and His254, which are involved in substrate binding and orientation, were also included in the model. Hydrogen atoms were added manually, and the amino acids were truncated so that in principle only side chains were kept in the model (see Figure 2). Truncated bonds were saturated with hydrogen atoms. The resulting active-site model is thus composed of 118 atoms and has a total charge of +1. To keep the optimized structures close to those obtained experimentally, the truncation atoms were fixed to their corresponding positions from the X-ray structure. The fixed atoms are marked with asterisks in Figures 2, 3 and 5.

Results and Discussion

The optimized structure of the dihydroorotase active-site model in which the dihydroorotate substrate is bound is shown in Figure 2. This structure will be termed Re (for re-

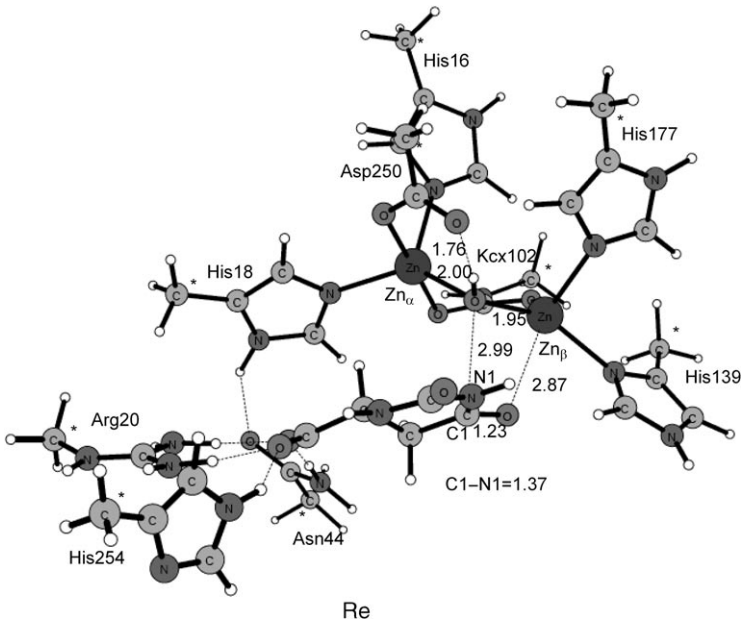

Figure 2. Optimized structure of the DHO active-site model bound to dihydroorotate (Re). Atoms marked with asterisks were fixed at their X-ray structure positions. Distances are given in Å.

actant) and all of the energies of the reaction will be compared with the energy of this structure. The overall geometric parameters obtained from the geometry optimization reproduce the experimental structure quite well. For example, the distance between the two zinc centers is calculated to be 3.41 Å, which is in excellent agreement with the crystallographic distance of 3.46 Å, and the hydrogen bond between the bridging hydroxide and Asp250 is well-reproduced. One slight disagreement, however, is that the calculations predict two symmetric bonds between the bridging hydroxide and the two Zn ions (2.00 and 1.95 Å to Zn_α and Zn_β, respectively), whereas the crystal structure shows some asymmetry (2.05 and 2.37 Å to Zn_α and Zn_β, respectively).

As seen from Figure 2, no significant interaction is observed between the substrate and the zinc ions. The distance between the carbonyl oxygen atom and Zn_β is 2.87 Å, which is very close to the distance found in the crystal structure (2.91 Å).[6] Instead, the substrate interacts with the side chains of the Arg20, Asn44, and His254 residues through a number of hydrogen bonds to the α-carboxylate group of dihydroorotate. These interactions help orient the substrate such that it is ready for nucleophilic attack, which is the first step of the suggested reaction mechanism. The distance between the bridging hydroxide and the carbon of the amide bond is 2.99 Å (2.79 Å in the crystal structure).

The optimized transition state for the nucleophilic attack (TS1) and the resulting tetrahedral intermediate (Int1) is shown in Figure 3. The barrier is calculated to be 13.5 kcal mol^{-1} (17.5 kcal mol^{-1} without the solvation correction), and Int1 is found at +11.5 kcal mol^{-1} (+16.5 kcal mol^{-1} without the solvation correction). We find that the nucleophilic attack happens directly from the bridging position. At TS1, the critical O_μ–C distance is 1.75 Å, which is dramatically decreased from 2.99 Å in Re, and the amide C–N and C–O bonds are elongated from 1.37 and 1.23 Å, to 1.40 and 1.31 Å, respectively.

At Int1, the bridging hydroxide asymmetrically binds to the two zinc ions (Zn_α–O_μ=2.10 Å, Zn_β–O_μ=2.42 Å). The resulting oxyanion of the carbonyl group binds to Zn_β with a bond length of 1.97 Å. This demonstrates that Zn_β provides electrostatic stabilization for the transition state and intermediate, thereby lowering the barrier for this reaction step. In addition, the decrease in the hydrogen-bond length between Asp250 and the bridging hydroxide from 1.76 Å in Re to 1.52 Å in Int1 implies that Asp250 also plays an important role in stabilizing the tetrahedral intermediate. Thus, in contrast with previous suggestions,[8] no proton transfer occurs during the nucleophilic attack step. Instead, the calculations suggest that this proton transfer takes place in a separate step.

We have managed to optimize a transition state in which the proton is transferred from the bridging oxygen to Asp250, coupled with the rotation of the latter to form a hydrogen bond to the amide nitrogen (TS2 in Figure 3). The nature of TS2 was confirmed to have an imaginary frequency of 137i cm^{-1}, which mainly corresponds to the swinging of the OH group in Asp250. TS2 is 7.0 kcal mol^{-1} higher in energy than Int1 (+18.5 kcal mol^{-1} relative Re) and the resulting new intermediate Int2 is only 0.1 kcal mol^{-1} lower in energy than TS2. In going from Int1 to Int2, the length of the scissile C–N bond increases from 1.44 to 1.53 Å. The proton transfer from the hydroxide to Asp250 weakens the coordination of Asp250 with Zn_α, as evidenced by the longer $O_{\delta 2}$–Zn_α distance (from 2.12 Å in Int1 to 2.31 Å in Int2). Furthermore, this proton transfer results in a dianionic bridging oxygen, which induces some contraction of the binuclear center, confirmed by a decrease in the Zn–Zn distance from 3.61 Å in Int1 to 3.47 Å in Int2.

The next step is the protonation of the nitrogen, which is coupled with C–N bond cleavage. The transition state for this step was located (called TS3, see Figure 3) and was confirmed to have an imaginary frequency of 808i cm^{-1}. At TS3, the scissile C–N bond is 1.59 Å, slightly increased from 1.53 Å in Int2. The critical O–H and H–N distances are 1.21 and 1.31 Å, respectively. This step is calculated to be the rate-limiting step of the whole reaction with an accumulated barrier of 19.7 kcal mol^{-1} (22.4 kcal mol^{-1} without the solvation correction) relative to Re (see Figure 4). This finding is consistent with the experimental solvent deuterium isotope effects that were measured to be around 2.1 for both directions of the reaction, which indicates proton transfer in the rate-limiting step.[8] These results are also consistent with the ^{13}C and ^{15}N heavy atom isotope effects that have been measured for the hydrolysis of dihydroorotate from *Bacillus caldolyticus*.[14]

The resulting product (Pr, see Figure 3) corresponds to the enzymatic binuclear zinc cluster in complex with the product carbamoyl aspartate. The energy of Pr is calculated to be 2.8 kcal mol^{-1} higher than Re (+6.5 kcal mol^{-1} without

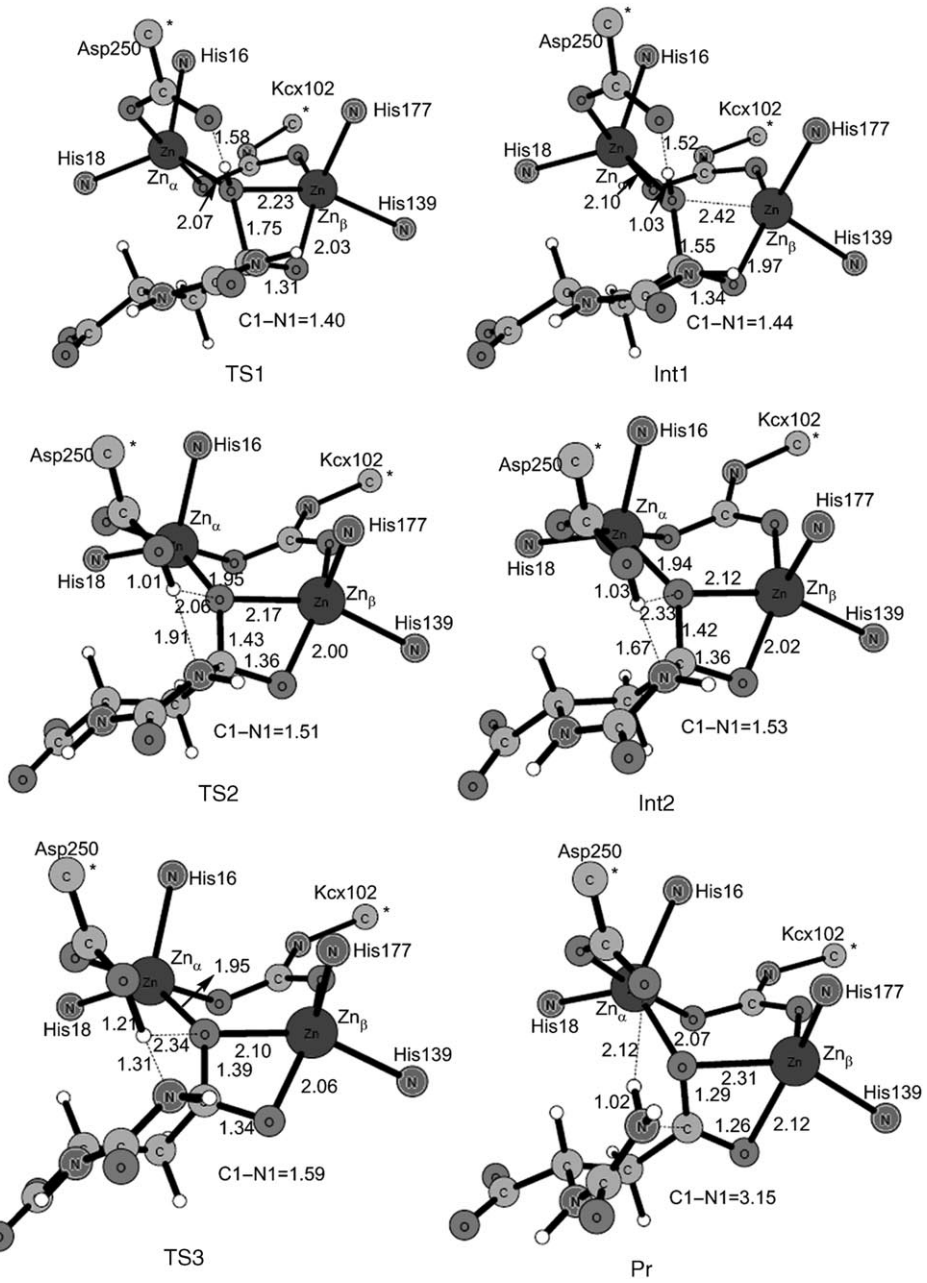

Figure 3. Optimized geometries for the transition states, intermediates, and product along the reaction pathway. For clarity, Arg20, Asn44, His254, the histidine rings, and unimportant hydrogen atoms are omitted

the solvent correction). Experimental rate constants for this reversible reaction are 160 s^{-1} with carbamoyl aspartate as the substrate at pH 5.8, and 100 s^{-1} with dihydroorotate as the substrate at pH 8.0.[8] This small difference in rate constants between the forward and reverse reactions indicates that the reaction is very close to thermoneutral. In this context, the calculated overall endothermicity of 2.8 kcal mol^{-1} must be considered very satisfactory.

The model calculations predict the geometry of the product species to have the carboxylate moiety of the carbamoyl aspartate binding bidentately to Zn_β and bridging the two zinc ions with one of its oxygen atoms. The crystal structure of this species shows, however, a somewhat different picture in which the carboxylate binds with one oxygen to each zinc. The most probable reason for this discrepancy in the structure of Pr is the procedure we use to lock the truncation atoms to their crystallographic positions (of the reactant state in this case). Of course this constraint limits the flexibility of the residues somewhat. It is, however, a necessary procedure without which the different parts of the active site will make large artificial movements that will render the model unrealistic and useless. Furthermore, the constraints have in general similar effects on all stationary points of the reaction, which makes the calculated relative energies rather insensitive to the constraints.[15]

To summarize, the reaction mechanism suggested by the calculations presented above is shown in Scheme 2, and the obtained potential-energy curve for the entire reaction is shown in Figure 4.

Protonation state of Asp250: The above calculations assume that the Asp250 residue is deprotonated in the resting state of the enzyme. It can, however, be envisioned that this residue is in the protonated form. We have in the present work explicitly considered this possibility. Accordingly, the reaction mechanism was investigated with Asp250 in the protonated form. The total charge of the active-site model becomes +2.

It turned out that with an extra proton residing on Asp250, the entire reaction takes place in one single concerted step in which the bridging hydroxide performs the nucleophilic attack on the amide carbonyl, the proton of Asp250 transfers to the amide nitrogen, and the C–N bond is cleaved simultaneously at the same transition state (called TS-pt and shown in Figure 5). Frequency analysis confirmed that the transition state had an imaginary frequency of 961 i cm^{-1}. Most importantly, the barrier for this mechanism is calculated to be 34.0 kcal mol^{-1} (28.3 kcal mol^{-1} for the reverse reaction, Figure 6). This is 14.3 kcal mol^{-1} higher in

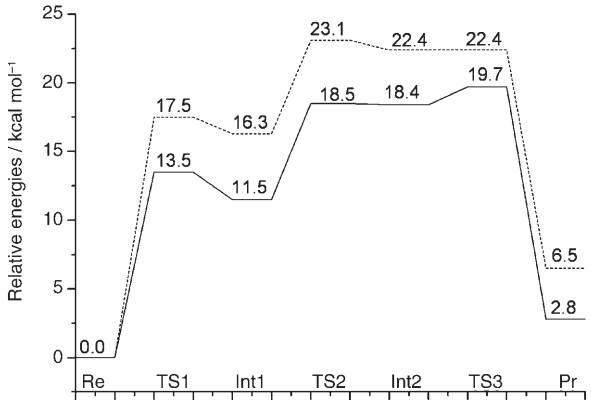

Figure 4. Calculated potential-energy curve for the hydrolysis of dihydroorotate by dihydroorotase; cluster + CPCM ($\varepsilon = 4$; ——), cluster(-----).

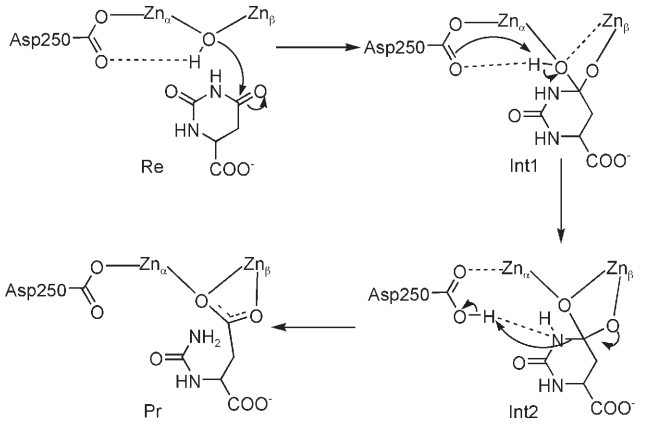

Scheme 2. Suggested dihydroorotate hydrolysis mechanism from the calculations.

energy than the mechanism in which Asp250 is deprotonated, and thus, rules out the possibility of performing the hydrolysis reaction with the extra proton at the active site.

Conclusion

We have in the present paper investigated the reaction mechanism for the binuclear zinc enzyme dihydroorotase by using a model of the active site. The potential-energy profiles were calculated by means of DFT methods. The energies obtained are presented in Figures 4 and 6 and important optimized geometric parameters of the stationary points are summarized in Table 1. Based on these calculations, the following conclusions can be drawn about the reaction mechanism of DHO:

1) Dihydroorotate binds the active site mainly through hydrogen-bond interactions with Arg20, Asn44, and His254, and it is not coordinated to Zn_β prior to nucleophilic attack by the bridging hydroxide.

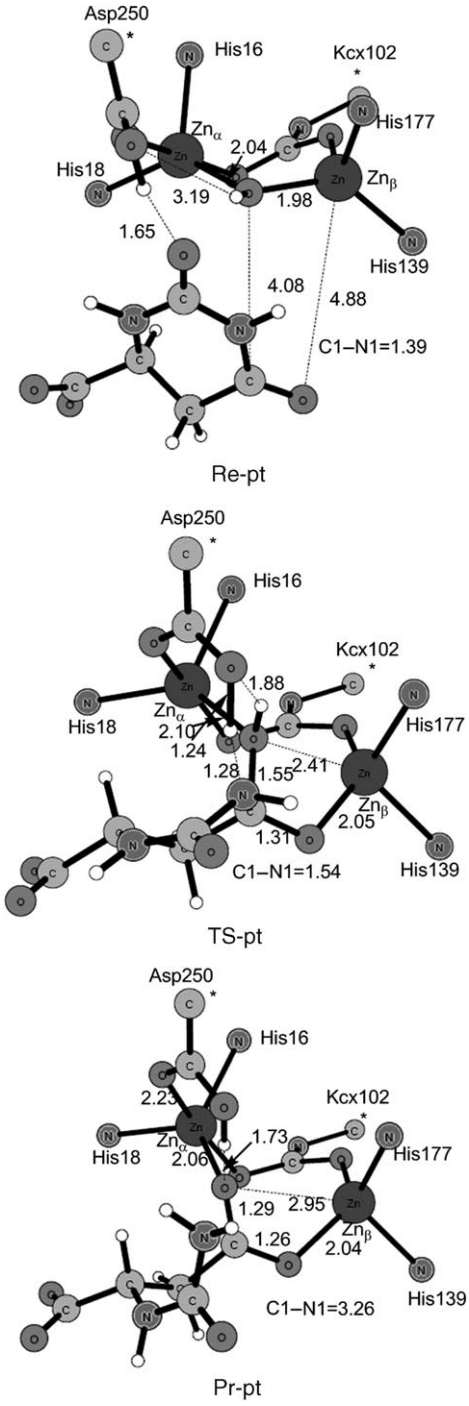

Figure 5. Optimized geometries for the reactant (Re-pt), the transition state (TS-pt), and the product (Pr-pt) along the reaction pathway in which Asp250 is protonated. For clarity, Arg20, Asn44, His254, the histidine rings, and unimportant hydrogen atoms are omitted.

2) The bridging hydroxide is capable of performing the nucleophilic attack from its bridging position without the need to become terminal. Zn_β catalyzes the reaction by stabilizing the transition state and the resulting oxyanion, thereby lowering the barrier for the nucleophilic attack.

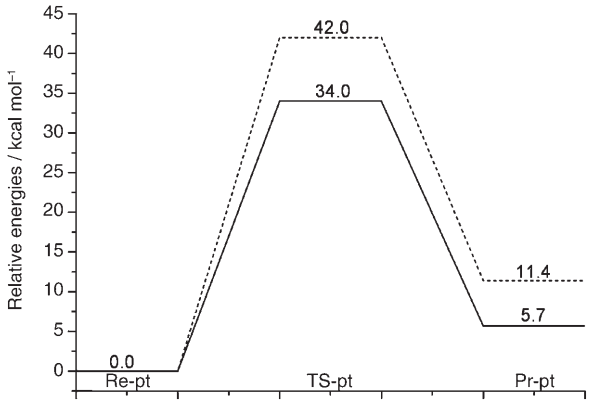

Figure 6. Calculated potential-energy curve for the hydrolysis of dihydroorotate in which the active-site Asp250 is protonated; cluster+CPCM ($\varepsilon=4$; ——), cluster (-----).

Table 1. Important distances [Å] for the various stationary points along the reaction pathway.

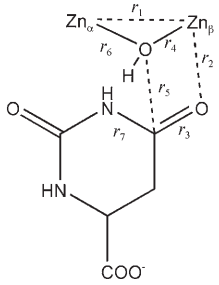

	r_1	r_2	r_3	r_4	r_5	r_6	r_7
Re	3.41	2.87	1.23	1.95	2.99	2.00	1.37
TS1	3.52	2.03	1.31	2.23	1.75	2.07	1.40
Int1	3.61	1.97	1.34	2.42	1.55	2.10	1.44
TS2	3.44	2.00	1.36	2.17	1.43	1.95	1.51
Int2	3.47	2.02	1.36	2.12	1.42	1.94	1.53
TS3	3.52	2.06	1.34	2.10	1.39	1.95	1.59
Pr	3.65	2.12	1.26	2.31	1.29	2.07	3.15
Re-pt	3.46	4.88	1.22	1.98	4.08	2.04	1.39
TS-pt	3.85	2.05	1.31	2.41	1.55	2.10	1.54
Pr-pt	3.86	2.04	1.26	2.95	1.29	2.06	3.26
Re[a]	3.46	2.91	1.22	2.37	2.79	2.05	1.40
Pr[a]	3.73	2.22	1.27	2.86	1.27	2.27	2.78

[a] Experimental X-ray structure values.

3) The rate-limiting step is the protonation of the amide nitrogen atom coupled with C–N bond cleavage. The reaction is calculated to be almost thermoneutral (+2.8 kcal mol^{-1}). The energetic barrier for the forward reaction is calculated to be 19.7 kcal mol^{-1}, whereas for the reverse reaction it is 15.9 kcal mol^{-1}.
4) The barrier of the reaction is much higher when the active-site Asp250 is protonated than when it is deprotonated. This result eliminates the possibility of protonated Asp250 prior to the binding of dihydroorotate.

Acknowledgements

F.H. gratefully acknowledges financial support from The Swedish National Research Council, The Wenner-Gren Foundations, The Carl Trygger Foundation, and The Magn Bergvall Foundation. This work was also supported by grants from the National Natural Science Foundation of China (Grant Nos. 20573011 and 20733002) and Major State Basic Research Development Programs (Grant Nos. 2004CB719903 and 2002CB613406). NIH support (GM71790) to F.M.R. is also gratefully acknowledged.

[1] a) M. W. Washabaugh, K. D. Collins, *J. Biol. Chem.* **1984**, *259*, 3293–3298; b) R. I. Christopherson, S. D. Lyons, *Med. Res. Rev.* **1990**, *10*, 505–548; c) M. E. Jones, *Annu. Rev. Biochem.* **1980**, *49*, 253–279.
[2] J. Brooke, E. Szabados, S. D. Lyons, R. J. Goodridge, M. C. Harsanyi, A. Poiner, R. I. Christopherson, *Cancer Res.* **1990**, *50*, 7793–7798.
[3] L. Holm, C. Sander, *Proteins: Struct. Funct. Genet.* **1997**, *28*, 72–82.
[4] C. M. Seibert, F. M. Raushel, *Biochemistry* **2005**, *44*, 6383–6391.
[5] S. B. Hong, F. M. Raushel, *Biochemistry* **1996**, *35*, 10904–10912.
[6] J. B. Thoden, G. N. Phillips, Jr., T. M. Neal, F. M. Raushel, H. M. Holden, *Biochemistry* **2001**, *40*, 6989–6997.
[7] M. Lee, C. W. Chan, J. M. Guss, R. I. Christopherson, M. J. Maher, *J. Mol. Biol.* **2005**, *348*, 523–533.
[8] T. N. Porter, Y. Li, F. M. Raushel, *Biochemistry* **2004**, *43*, 16285–16292.
[9] a) A. D. Becke, *J. Chem. Phys.* **1993**, *98*, 5648–5652; b) C. Lee, W. Yang, R. G. Parr, *Phys. Rev. B* **1988**, *37*, 785–789.
[10] a) F. Himo, P. E. M. Siegbahn, *Chem. Rev.* **2003**, *103*, 2421–2456; b) L. Noodleman, T. Lovell, W.-G. Han, J. Li, F. Himo, *Chem. Rev.* **2004**, *104*, 459–508; c) P. E. M. Siegbahn, T. Borowski, *Acc. Chem. Res.* **2006**, *39*, 729–738; d) F. Himo, *Theo. Chem. Acc.* **2006**, *116*, 232–240; e) S.-L. Chen, W.-H. Fang, F. Himo, *J. Phys. Chem. B* **2007**, *111*, 1253–1255; f) S.-L. Chen, T. Marino, W.-H. Fang, N. Russo, F. Himo, *J. Phys. Chem. B* **2008**, *112*, 2495–2500..
[11] P. J. Hay, W. R. Wadt, *J. Chem. Phys.* **1985**, *82*, 270–283.
[12] a) V. Barone, M. Cossi, *J. Phys. Chem. A* **1998**, *102*, 1995–2001; b) R. Cammi, B. Mennucci, J. Tomasi, *J. Phys. Chem. A* **1999**, *103*, 9100–9108; c) A. Klamt, G. Schüürmann, *J. Chem. Soc. Perkin. Trans. 2* **1993**, 799–805; d) J. Tomasi, B. Mennucci, R. Cammi, *Chem. Rev.* **2005**, *105*, 2999–3094.
[13] Gaussian 03, Revision D.01, M. J. Frisch, G. W. Trucks, H. B. Schlegel, G. E. Scuseria, M. A. Robb, J . R. Cheeseman, J. A. Montgomery, Jr., T. Vreven, K. N. Kudin, J . C. Burant, J. M. Millam, S. S. Iyengar, J. Tomasi, V. Barone, B. Mennucci, M. Cossi, G . Scalmani, N. Rega, G. A. Petersson, H. Nakatsuji, M. Hada, M. Ehara, K. Toyota, R. Fukuda, J . Hasegawa, M. Ishida, T. Nakajima, Y. Honda, O. Kitao, H. Nakai, M. Klene, X. Li, J. E. Knox, H. P. Hratchian, J. B. Cross, C. Adamo, J . Jaramillo, R . Gomperts, R. E. Stratmann, O. Yazyev, A. J. Austin, R. Cammi, C. Pomelli, J. W. Ochterski, P. Y. Ayala, K. Morokuma, G . A. Voth, P . Salvador, J. J. Dannenberg, V. G. Zakrzewski, S . Dapprich, A. D. Daniels, M. C. Strain, O. Farkas, D . K. Malick, A. D. Rabuck, K. Raghavachari, J. B. Foresman, J. V. Ortiz, Q. Cui, A. G. Baboul, S. Clifford, J. Cioslowski, B. B. Stefanov, G. Liu, A. Liashenko, P . Piskorz, I. Komaromi, R. L. Martin, D. J. Fox, T. Keith, M. A. Al-Laham, C. Y. Peng, A. Nanayakkara, M. Challacombe, P. M. W. Gill, B. Johnson, W. Chen, M. W. Wong, C. Gonzalez, J. A. Pople, Gaussian, Inc., Pittsburgh, PA, **2004**.
[14] M. A. Anderson, W. W. Cleland, D. T. Huang, C. Chan, M. Shojaei, R. I. Christopherson, *Biochemistry* **2006**, *45*, 7132–7139.
[15] V. Pelmenschikov, M. R. A. Blomberg, P. E. M. Siegbahn, *J. Biol. Inorg. Chem.* **2002**, *7*, 284–298.

Received: December 8, 2007
Published online: March 25, 2008

